A Report to ONR-D3D project
work duration: 17 weeks
(%33 work load of Aug05-March06+ %60Dec06+50March07)

THE EFFECTS OF INCLUSION INTERFACIAL ADHESION ON CRACK TIP BEHAVIOR AND FRACTURE TOUGHNESS

S. Hao[a]

[a]**Department of Mechanical Engineering**
Northwestern University
2145 Sheridan Rd., Evanston, Illinois, 60208

[a]**suhao@northwestern.edu**

ABSTRACT

A study has investigated the roles of inclusion cracking and interfacial debonding in the ductile fracture of a high-strength martensitic steel. Focused on the effects of second phase particles and segregates of impurities, computations of interfacial adhesion at quantum scale and micro-scale cell model with breakable inclusions have been performed, in conjunction with slip-line fields and dislocation analysis. It concludes that high interfacial adhesion benefits both strength and fracture toughness. Large inclusions with coherent interface reinforces matrix. However, in the presence of inclusion cracking, interfacial separation accelerates primary void growth, lowering toughness in agreement with recent experiments. The performed series of quantum mechanical computations quantify the effects of Sulfur segregation. It has been found that small Calcium-Sulfide (CaS) belongs to the family of semi-coherent particles with minor misfit to bcc iron matrix, which extract Sulfur atoms from segregation and thus may improve the interfacial properties between TiN inclusions and iron matrix.

1. INTRODUCTION

Ductile fracture of an alloy can be phenomenologically divided into three stages: stress and strain concentration that results in onset of strain localization; separation of the material creating new surfaces to form micro cracking and/or voids; the coalescence of

these damages that leads to failure at macroscales. In the first stage, highly concentrated stress-strain state focuses energy into very small regions with heterogeneities in alloy's matrix, e.g., inclusions and grain boundaries. The subsequent separation highlights the underlying mechanisms at micro and quantum scales, dominating the following damage evolution and macroscale fracture. The nucleation sites of such material's separations and the adhesions between new-created surfaces are the two factors that essentially govern the process of ductile fracture [1,3,4].

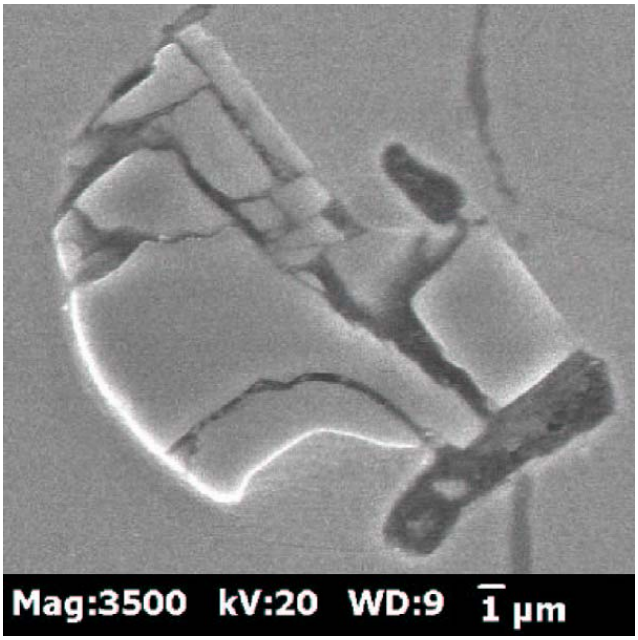

Fig. 1 A broken TiN inclusion with interfacial separation to steel matrix [2]

On other hand, for many martensitic steels and other low-alloy ultra-high strength steels, dispersed small M_2C/MC particles(precipitates) with the associated "precipitate hardening is a dominant mechanism to gain superior strength; where "M" refers to the transition metal's elements, such as V, W, Ti, Cr, Nb, which are used as microalloy additions to form nanometer-sized carbides in iron matrix to pin dislocations and so as to elevate resistance against lattice's slipping, leading to higher strength. Among these elements, titanium (Ti) is an effective addition for the ultra-high strength steels under a wide range of working temperatures with many other advantages. However, it has been observed that titanium and the nitrogen solved in alloy matrix also form titanium nitride (TiN) during both solution and isothermal treatments. Although small TiN particle has the similar coherence to iron matrix as TiC; the relatively high thermodynamic stability allowing the continuous growth of TiN that extracts titanium atoms through dissolving Ti-carbides, which leads to micron-sized large breakable TiN particles. Impurity elements, particularly Sulfur (S), may segregate at its boundary to iron matrix, resulting in significant deduction of interfacial adhesion. Under this situation, both the fracture of large TiN particles and the TiN-iron interfacial separation promote the process of damage-nucleation, growth and coalescence, which detriments strength and toughness of

the steel simultaneously, see Fig. 1. Beside the controlling of the size, strength and toughness of TiN particles, the interfacial adhesion to iron matrix becomes crucial for its mechanical properties.

Hence, an effective way among many others to improve the mechanical properties of steels is to remove undesirable impurity elements such as Sulfur and Phosphorous when large grains and primary inclusions like TiN are not evitable. For Sulfur, the mineral element Calcium (Ca) from limestone is a conventional microalloy addition that is put into melted iron to extract acidic oxides and sulfur, so as to form Ca-based compounds that run to bottom of the furnace. In recent years, an increasing number of research reports indicate that overdosed Calcium (Calcium-treated steels) and more Mg can achieve improved mechanical properties and better corrosion-resistance [5,6].

Another “abstraction” mechanism to purify alloys has been suggested in [7], which indicates that formations of some semi-coherent intermetallic compounds through microalloying is another way to abstract harmful impurities from interfaces. For retard Sulfur, the Alkaline Earths elements (the group II in chemical periodic table) Magnesium (Mg) and Calcium(Ca) are the two candidates for this purpose. Mg or Ca atom is generally intending to establish covalent bonding with S atom through forming closed d-shell of electrons by hybridization, resulted in the rock-salt structured crystals like MgS or CaS. The enhanced extraordinary chemical stability enables them to extract sulfur atoms from interface surfaces. This mechanism explains the phenomenon that Ca “globalizes” Sulfur observed in [5,6]. Also, the small binary compound MgS also triggers the austenite to martensite transformation which induces more uniformly-dispersed martensite nucleation sites. However, large MgS particles have been also frequently observed as the sources of brittle fracture. In this study we will focus on Calcium.

The Sulfur interfacial segregation and formations of (Ca,Mg)S compounds are two competing mechanisms. Experimental studies indicate that the cooling rate after solution treatment plays is vital important for the diffusion-segregation. An example is the modified 4340, i.e. the E1371 steel developed by Caterpillar Corp.[2,8]; which is a class of ultra-high strength, medium carbon, low-alloy martensitic steels for construction and mine heavy machines under dynamic loads. A feature in the microstructure of this class steels is the presentations of remarkable amount of large microvoids after ductile fracture, initiated by the interfacial debounding of cubic TiN inclusions with the size around 0.2-10 microns. On another hand, this class of steels demonstrates remarkable high strength and fracture toughness when the matrix and interfaces to the inclusions are strong enough. Figs. 2a and 2b are the microscale fractographies of two groups of modified 4340 steels with the same chemical composition but with different cooling rates during the quenching process after solution treatment. Fig. 2a is the group with oil quenching, which shows remarkable Sulfur concentration in the areas around the TiN boundaries. As contrast, the fractographies of water quenched specimens are given by Fig. 2b that includes two subgroups: the subgroup I exhibits dispersed Sulfur in iron matrix whereas the subgroup II shows both Sulfur and Calcium segregates along the

interface. The corresponding fracture toughness is about 30% higher than the oil quenched case. These observations confirm the speculation that Sulfur segregation is a cause of lower ductility. However, it is not clear the function of retard Ca addition to interfacial adhesion when Sulfur segregation presents, as shown in the subgroup II of Fig.3.

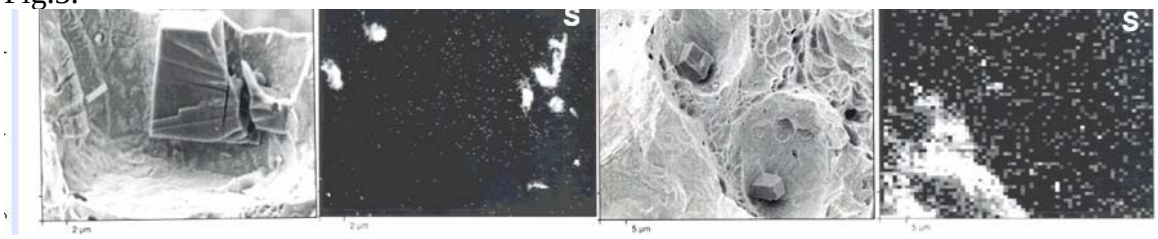

(a) oil-quenched specimen: broken TiN particles with concentration of sulfur atoms at interface

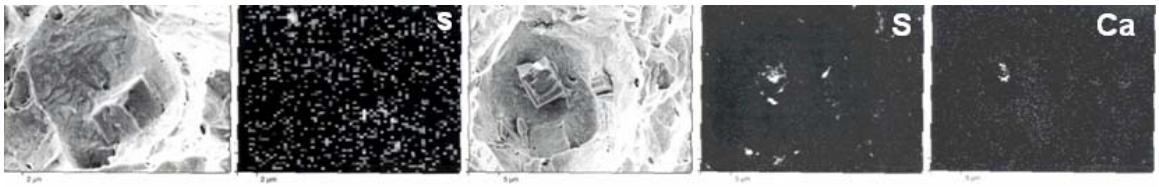

Subgroup I Subgroup II

(b) water quench specimen: broken TiN particles with dispersed S or with S and Ca segregations

Fig. 2 Fractographies of broken TiN particles and the measurements of the corresponding Sulfur distributions [8]

Based on the experimental results of modified 4340 steels, in this paper a computational study has been performed focused on the following two tasks: (i) a series quantum mechanics computations to identify the adhesion between TiN inclusion and bcc steel matrix with Sulfur segregation and to explore the effects of microalloy additions such as Calcium; these computational results provide the bases for the next task: (ii) a microscale parametrical studies by representative cell and crack models, finding the quantitative relationship between interfacial adhesion and the strength of TiN inclusions and their effects on the alloy's macroscale mechanical behavior. The damage-based constitutive law with Needleman-Tvergaad's void nucleation and growth theory [9-11], in conjunction with computational results, has been applied to describe the phenomena of macroscale ductile fracture.

2. Sub-atomic Scale Analysis: Interfacial Adhesion and Effects of Microalloys

To quantify the effects of Sulfur segregation needs sub-atomic scaled analysis of the TiN-S-Fe crystalline system through solving Schrödinger's equation. The Density-Functional Theory [12,13] (DFT)-based procedure with the linear argument plane wave (lapw) technique [14-16] has been applied for obtaining the numerical solutions. The analysis are performed under ground state.

The TiN particles usually have the diameters in the order of 0.2-10 nanometers; hence a TiN-Fe crystalline system contains 10^{10} to 10^{21} atoms. It is beyond the current computational capability to compute the numerical Schrödinger's solution for such a big structure and the microstructure displayed in Figs. 1-3, a multi-scale model as demonstrated in Fig. 4 is proposed to set up the boundary value problem for the quantum mechanical computation. In this procedure, the first step is to approximate the matrix-particle system in (a,b) as an interface between the two half infinite mediums demonstrated in (c). Since the system (c) still need extreme computation effort, it has been further simplified as the laminate system (d) by assuming that the height of the layer is large enough so at each interface the effects from other layers are ignorable. Finally, by applying the periodicity of the system (d) we obtain the supercell with 67 atoms for the TiN-Fe interfacial computation, as plotted in (e). Due to periodicity, in this supercell only 30 atoms are independently presented in computation. By performing the computations for the supercell as Fig.4(e) and the cells split along the desirable interface, the derivative of the system's energy with respective to separation distance determinates the short range bonding force [20]. The detail process has been described in [3].

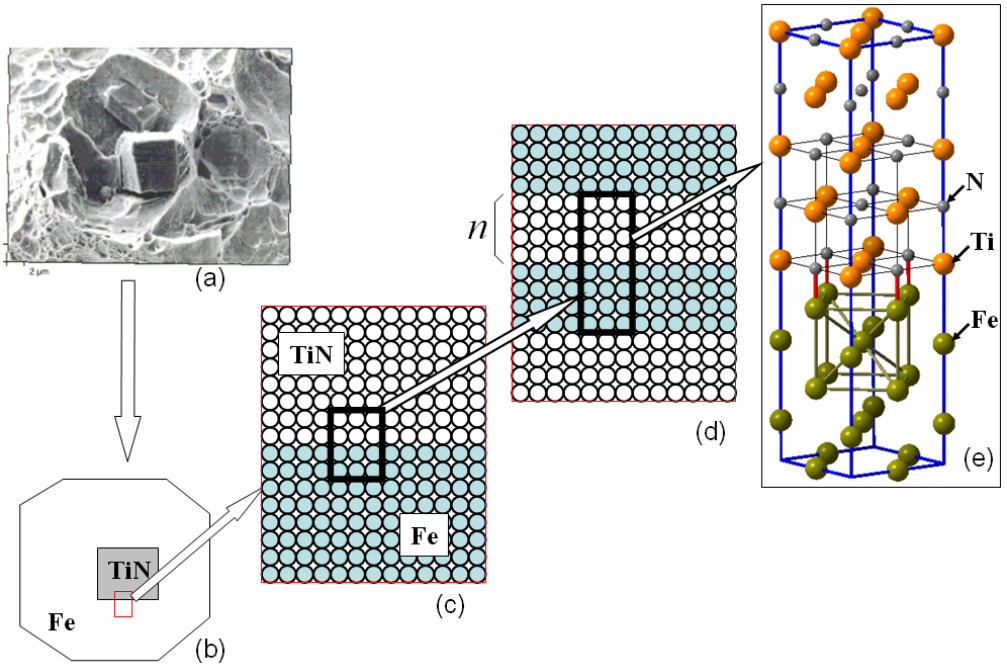

Fig. 3 Supercell set-up for quantum mechanical computation

Table I: Interfacial Adhesion $[001]_A$ //$[001]_B$

system	adhesion (J/M^2)
TiN// BCC-Fe with S segregate (substantial site to Fe; S-N site to TiN)	-1.91
TiN// BCC-Fe with S segregate (substantial site to Fe; S-Ti site to TiN)	0.75

TiN// BCC-Fe with S segregate (interstitial site to Fe, S-Ti site to TiN)	2.31
CaS// BCC-Fe	1.8041
TiN//CaS	1.47

In this paper the major conclusions with brief discussion will be given about the performed quantum mechanical computations. Listed in Tables I are the computed adhesion energies for various cases. Differing from conventional understanding, these results reveals that "weak" covalent bonds can be established between Sulfur atom and Fe atom on one side while Ti atom on another side when the Sulfur atom is near the tetrahedral interstitial site of BCC iron, as demonstrated by the third row of Table I. However, when Sulfur atom faces Nitrogen atom, the computation indicates an existing strong repulsive force between the two atoms at the equilibrium distance when an interstitial Sulfur atom faces Ti atom. This repulsive force degenerates and finally vanishes until the system releases the energy in the amount of 1.91Joul per M^2 of the interface surface; this is why a negative sign appears in the first row of the Table. Under this situation, the Sulfur segregation works in the same way as Hydrogen embrittlement which causes interfacial separation without applied external load. Listed in Table II are the lattice misfits between bcc iron matrix and different second phase particles, which indicates an about 8% misfit for TiN. Hence, in practical application it is usually very difficult to keep segregated Sulfur atoms from neighboring to Nitrogen atoms due to the misfit-induced dislocation. Consequently, the direct result of Sulfur segregation is of the reduction of interfacial adhesion.

Based on the experimental observations in past, the analysis and computations in this research reveal that retard Calcium atoms may benefit the steel's mechanical properties through the following two ways: (i) to form stable CaS compound stoichiometrically that extracts Sulfur from interface surface; (ii) instead of Sulfur segregation, the small CaS molecules may also segregates between iron matrix and TiN particles to glue the two phases. This is because the small misfits exist between CaS and bcc iron as well as between CaS and TiN, as demonstrated by Table II. On other hand, the performed computation indicates that weak chemical bonds can be established between CaS and either BCC iron or TiN. for both cases the corresponding adhesion energy is still greater than that with Sulfur segregation at substantial site, see Table I.

Plotted in Fig. 4a is the electron charge distribution of the TiN-bccFe interface with Sulfur segregation at interstitial position. In this figure one sees a half-moon shaped distribution on the both side of Sulfur atoms to Fe and Titanium atoms. It can be explained as the accumulated charge densities of 3*p*4*s* electrons between S and Fe on one side and S and Ti on another side. However, the 3*d* electrons in un-fully-filled out shell induce certain impel force towards enlarging the interatomic distances over the interface and the transverse lattice constants in iron matrix, weakening the covalent bonds built up by 3*p*4*s* mixing. Fig. 4b is the iso-valued surface of electron charge in CaS molecule,

where the continuous surface implies the established covalent bonds between atoms in this Rock-Salt structured crystal.

Table II: Lattice constants and misfit with bcc iron matrix

	TiC[16]	TiN[3]	CaS	MgS
lattice constant (A)	4.25	4.37	5.89	5.61
45^o misfit to bcc Iron (%)	5.07	8.04	45.1	38.7
0i^o misfit to bcc Iron (%)	48.4	52.3	**2.6**	**-2.3**
45^o misfit to TiN (%)			**4.93**	10.2

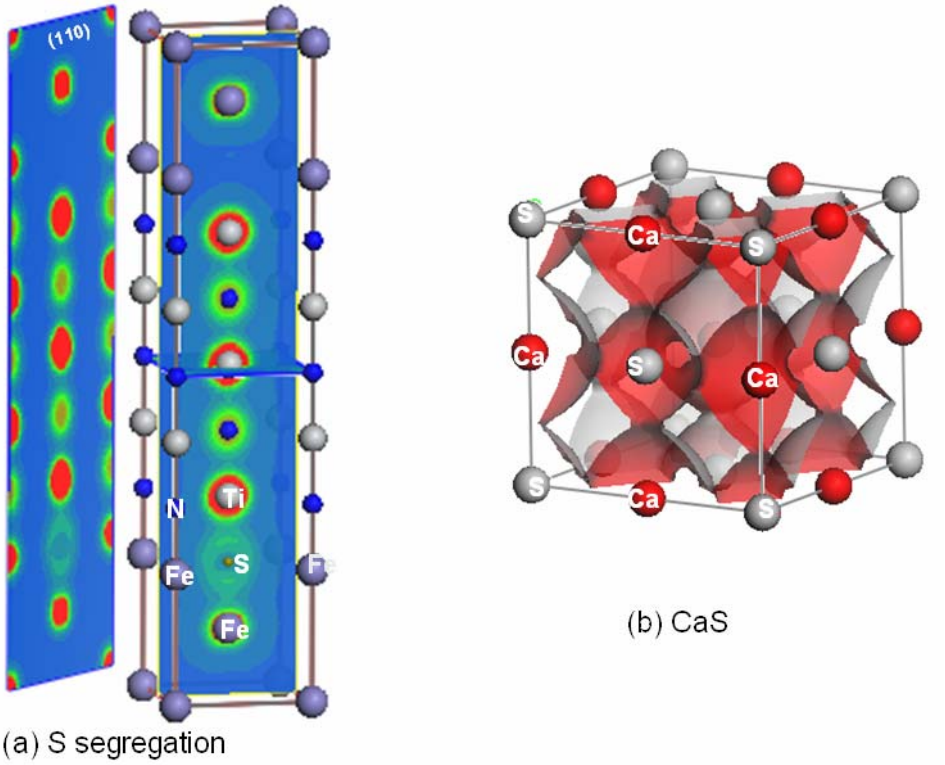

Fig. 4: (a) electron charge distribution of the TiN-bccFe interface with Sulfur segregation at interstitial position; (b) the iso-valued surface of electron charge distribution in Rock-Salt structured CaS crystal

3. Parametrical Study of Representative Cell Modeling with Varying Interface Adhesion and Strength of Inclusions

As indicated by the quantum mechanical computation in the previous section, the amplitude of TiN-BccFe interface adhesion may vary within a wide range. On other

hand, experimental observations evidence TiN particles to be brittle and breakable. In this section the two and three dimensional microscale representative volumetric element (cell) model illustrated in Fig. 5 has been adopted to investigate the effects of the strengths and their ratio κ_p on macroscale mechanical properties.

The Ramburg-Osgood relation has been applied to describe the equivalent stress-strain relation of the steel matrix in Fig. 5. According to well know crack tip field analysis [17], the hydrostatic stress reaches a maximum value (about 3.1 σ_Y) at a point ahead of the crack tip at a distance of 1.9 times the crack tip opening displacement. This is the location with the maximum driving force for void nucleation and growth [17,18]. Hence, in this study the hydrostatic load is taken as the outer boundary condition to the cell in Fig. 5. A critical normal stress for the TiN inclusion cracking at its center plane is taken from notched bar void nucleation measurements [2]. The cohesive zone force-distance law for particle/matrix interfacial separation are adopted from the computations introduced in the previous section with varying amplitudes. As illustrated by Fig. 6, five different volumetric ratios of the TiN particles, varying from 0.0001 to 0.008, have been analyzed. Fig. 7 is a 3D example with broken TiN and $\kappa_p = 0.6$. In all these analysis it is assumed that the iron matrix' strength and toughness are higher than that of both interface and inclusions.

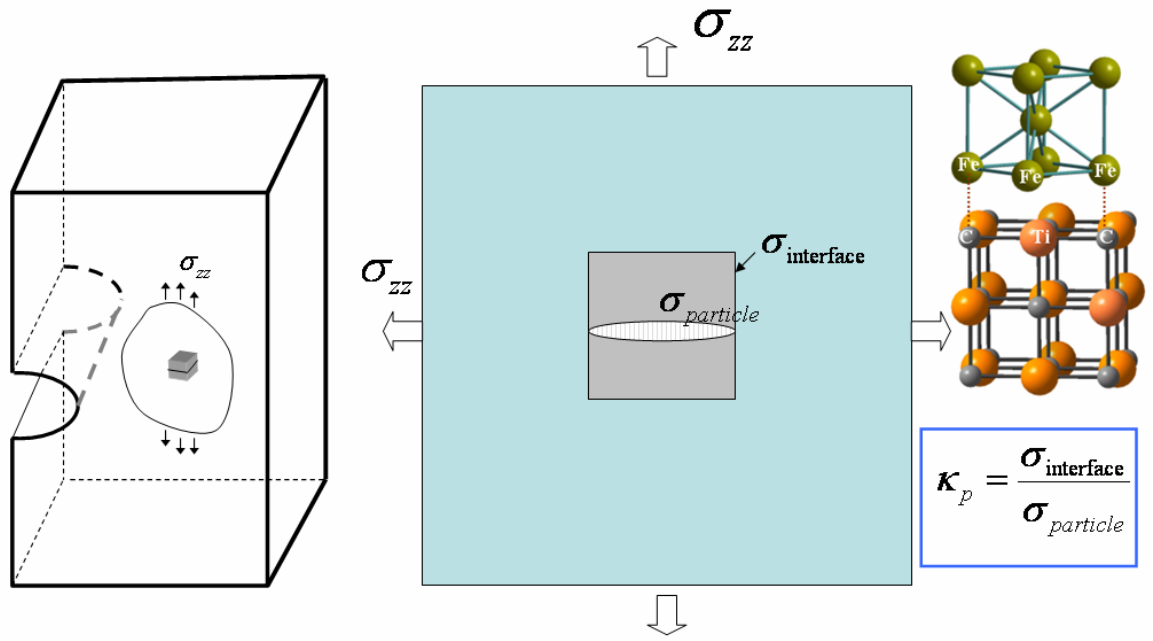

Fig. 5 The representative volumetric element (cell) modeling with breakable inclusion.

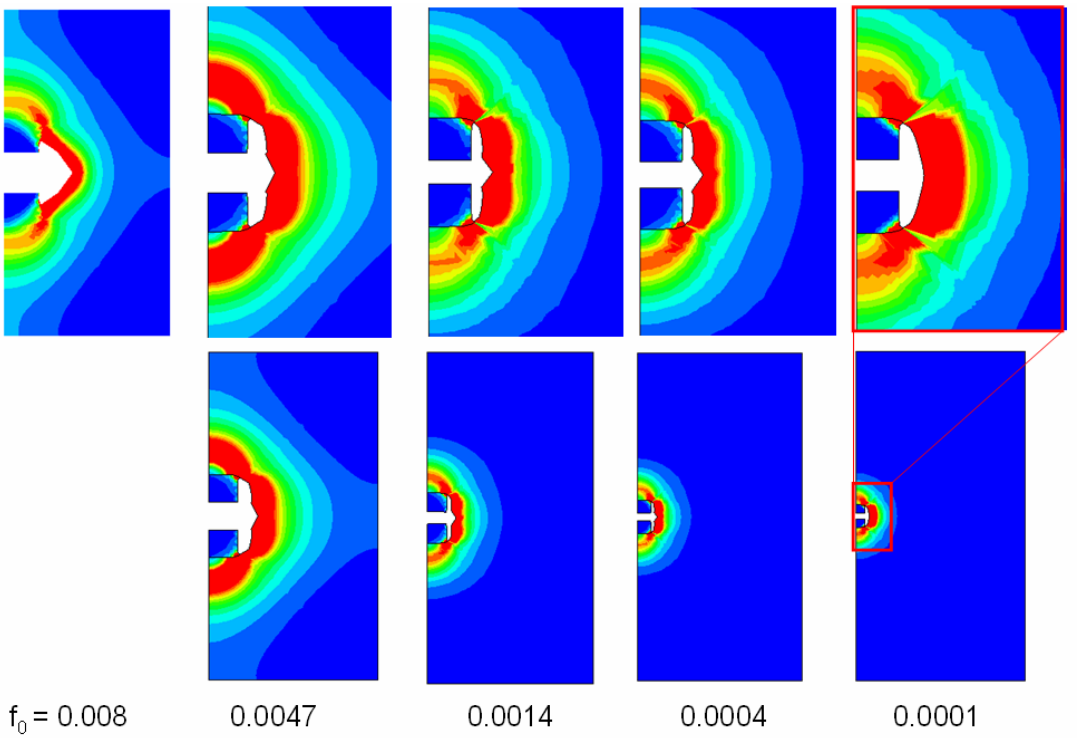

Fig. 6: Cell model with five volumetric ratios of TiN inclusion have been analyzed

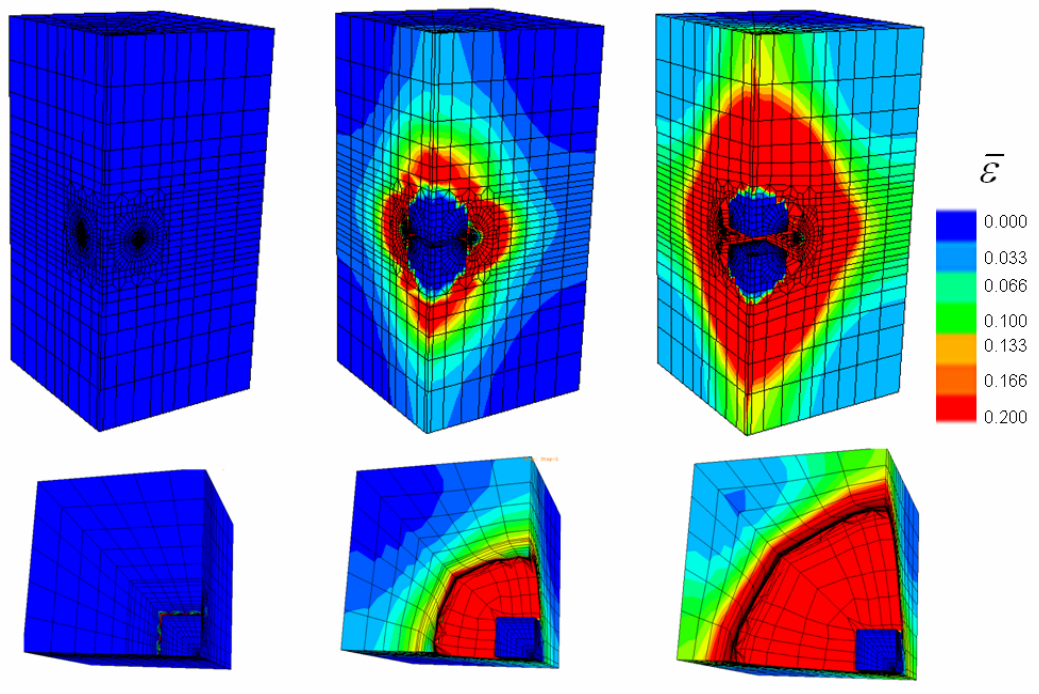

Fig. 7: A 3D example with breakable inclusion ($\kappa_p = 0.6$).

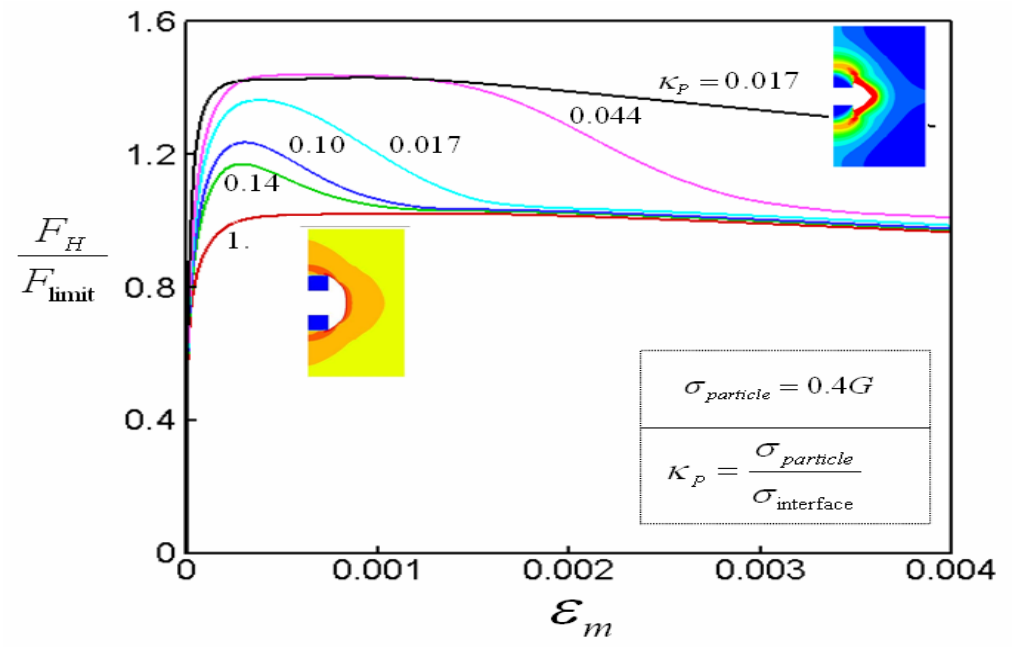

(a)

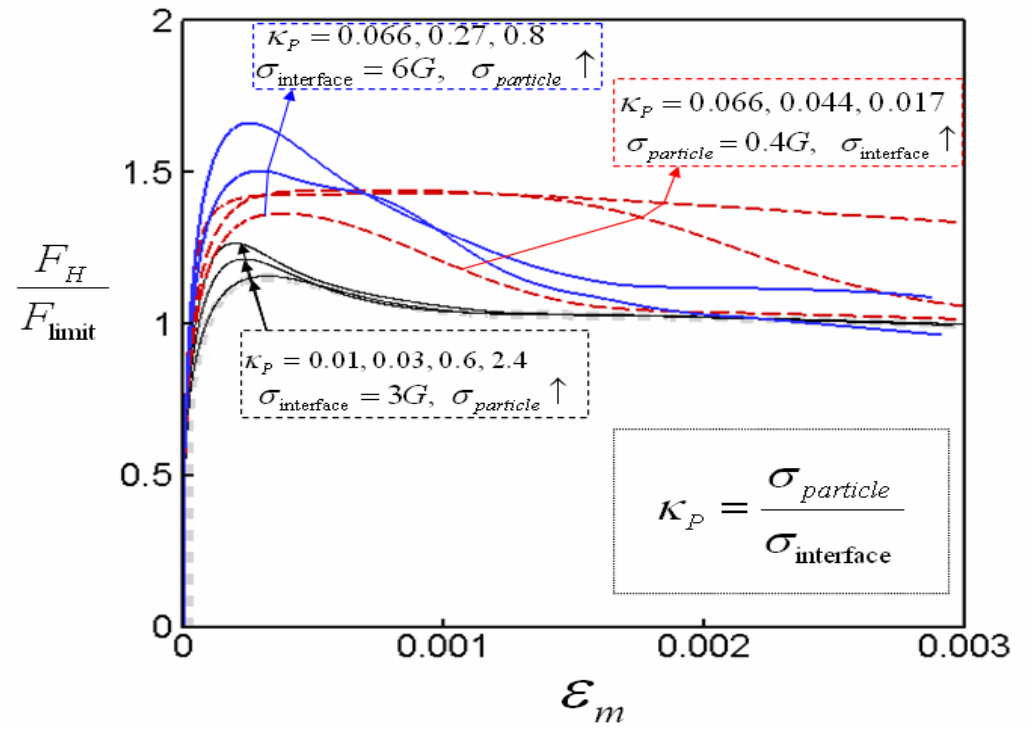

(b)

Fig. 8: The macroscale stress-strain curves when the ratio κ_p and interfacial strength vary; where F_{limit} is the plastic limit load of the cell.

As shown by the macroscale volumetric stress-strain curves in Figs. 8a,b and the associated void shapes, interfacial debonding significantly increases the evolution of void volume associated with inclusion cracking, with a corresponding reduction of the load carrying capacity of the representative cell. This is consistent with experimental observations correlating S segregation at the TiN interfaces with lower ductile fracture toughness attributed to easier interfacial separation. The results of Fig. 8b indicate that at higher interfacial adhesion, increasing the strength of inclusion results in higher "threshold" of the cell against applied load, followed by fast drop of load carrying capacity after interfacial debonding. Fig. 9 shows the trend demonstrated in Figs. 8a,b remains but with lower amplitude when the volume fraction of the inclusion is lower.

Since both interfacial debonding and inclusion broken can be counted as the nucleation of microvoids, the phenomena demonstrated by computational results can be described by the Chu-Needleman's damage nucleation mode [9]l:

$$\Delta f_{nucleation} = g_0\left(\frac{\sigma_m}{\sigma_y}, \kappa_p\right)\exp\left(-\left[\frac{\sigma_m - \min\left\{\sigma_{\text{interface}}, \sigma_{particle}\right\}}{s_N}\right]^2\right) \tag{1}$$

in conjunction with a simplified form of the generalized plastic potential [3]:

$$\Phi_{macro} = \left(\frac{\sigma_{eq}}{\sigma_{\text{intr}}}\right)^2 + f \cdot g_1\left(\frac{\sigma_m}{\sigma_y}, \kappa_p\right)\cosh\left(\frac{3\sigma_m}{2\sigma_{\text{intr}}}\right) - \left(q_0 + q_1(f)^2\right) = 0 \tag{2}$$

In (1,2) f is volume fraction of microvoids; σ_{eq} and σ_m stand for Von Mises and mean stress, respectively; s_N, q_0, q_1 are material's constants; the coefficient functions $g_0\left(\frac{\sigma_m}{\sigma_y}, \kappa_p\right)$, $g_1\left(\frac{\sigma_m}{\sigma_y}, \kappa_p\right)$ are to be calibrated by the computations, e.g. the results plotted in Figs. 8 and 9; The equation (2) can be considered as a generalized Gurson-Needleman-Tvargaard damage model [19].

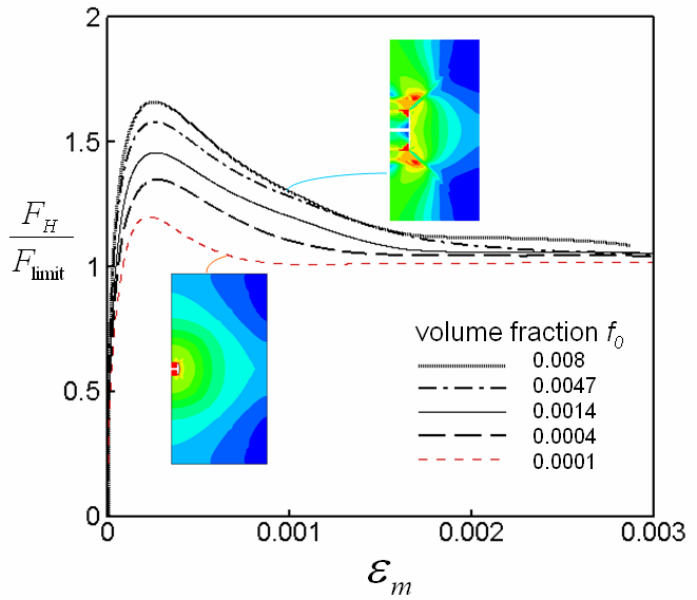

Fig. 9 Effects of inclusion volume fraction ($\kappa_p = 0.8$, $\sigma_{\text{interface}} = 6G$)

4. Conclusions

According to the conducted misfit/interfacial adhesion analysis at quantum scale and the microcell models with varying levels of interfacial adhesion, inclusion and matrix strengths, the following conclusions are obtained

1. For a steel made of iron matrix and pure elastic hard inclusion, its fracture toughness elevates when the interfacial adhesion increases. However, the increment of toughness is inversely proportional to the matrix strength. The relationships among these properties coincide to that indicated by the Toughness-Strength-Adhesion diagram in [3]
2. When the strength and toughness of the inclusion are lower than iron matrix, but the adhesion energy at the interface between inclusion and matrix is high, the overall mechanical behavior is governed by the matrix properties. Decreasing the interfacial adhesion energy results in the acceleration of voids nucleation from the inclusions, which reduces both strength and toughness.
3. As a competing mechanism to Sulfur interfacial segregation, certain retard Calcium addition may form stable CaS particles stoichiometrically. The CaS particles is semi-coherent to iron matrix with considerable stability, which can be either dispersed in iron matrix or segregated at the interface surfaces, such as that between TiN particle and Fe matrix, to “glue” the surfaces from both sides. Hence,

the formation of CaS reduces free Sulfur atoms segregation and hence improves the mechanical properties. A very recent experiment employing Ca treatment in the same steel to get S in a more stable form has demonstrated voiding by TiN cracking without significant interfacial separatiuon, with an associated significant enhancement of fracture toughness.

REFERENCES:

[1a] "Cybersteel 2020" - an ONR sponsored project of quantum steel design; project officer: Julia A Christodoulou; PI: G. B. Olson; Co-PIs: A Freeman, B. Moran, W.K. Liu (NWU).

[1b] "D3D" - an ONR sponsored project of quantum steel design; project officer: Julia A Christodoulou; PI: G. B. Olson; Co-PIs: A Freeman, B. Moran, W.K. Liu (NWU), D. Parks(MIT), D. McDowell(GIT)

[2a] Briant, C. L., Sylven, E., Shabrov, M. N., Sherman, D. H., Chuzhoy, L., and A. Needleman, 2004, "*Void Nucleation in a Low Alloy Steel*", Proc TMS Annual Meeting, TMS-AIME.

[2b] Sherman, D. H., Yang, N., Miller, M. K., Grandjean, F., and Long, G. J., '*3D Characterization of the Carbon Distribution in a Medium Carbon Steel*', to be published in Acta Materialia, 2007.

[3] Hao S., B. Moran, W. K. Liu, G. B. Olson, 2003, "*A Hierarchical Multi-Physics Model for Design of High Toughness Steels*", J. of Computer-aided Materials Design, 10(2), 99-142

[4] Hao, S. and W. Brocks, *The Gurson-Tvergaard-Needleman-model for rate and temperature-dependent materials with isotropic and kinematic hardening.* Computational Mechanics, 1997. **20**(1-2): p. 34-40.

[5] Brodetskii, I. L., Kharchevnikov, V. P., Belov, B. F., Trotsan, A. I., 1995, "*Effect of Calcium on Grain Boundary Embrittlement of Structural Steel Strengthed with Carbonitrides*", Metal Science and Heat Treatment, 37(5-6), 24-26.

[6] Dyudkin, D. A., Grinberg, S. E., et al, 2002, "*Effect of Calcium on the Quality of Tube Steel*", Metallurgist, **46**(11-12), 344-346.

[7] Hao, S., Lin, H., Binomiemi, B. *et al., "A Multi-Scale Model of Intergranular Fracture and Computer Simulation of Fracture Toughness of a Carburized Steel"* Proceedings of Int. Symp. Long Forge Products, Winter Park, 2006; submitted for publication.

[8] Hsieh, K. C., Doctorial Work, 2000-2004, Caterpiller Corp./Northwestern University.

[9] Chu, C. C. and Needleman, A., 1980, "Void Nucleation Effects In Biaxially Stretched Sheets", J. Eng. Mat. Tech., **102**, 249-256.

[10] Tvergaard, V. and A. Needleman, *Effect of Crack Meandering on Dynamic, Ductile Fracture.* Journal of the Mechanics and Physics of Solids, 1992. **40**(2): p. 447-471.

[11] Needleman, A., *A continuum model for void nucleation by inclusion debonding.* J. Appl. Mech., ASME, Trans, 1987. **54**(3): p. 525-531.

[12] Hohenberg, P., Kohn, W., *Inhomogeneous Electron Gas.* Physical Review, 1964. **136**(3B): p. 864-871.
[13] Kohn, W., Sham, L. J., *Self-Consistent Equations Including Exchange and Correlation Effects.* Physical Review, 1965. **140**(4A): p. 1133-1138.
[14] Wimmer, E., et al., *Full-Potential Self-Consistent Linearized-Augmented-Plane-Wave Method for Calculating the Electronic-Structure of Molecules and Surfaces - O2 Molecule.* Physical Review B, 1981. **24**(2): p. 864-875.
[15] NRL, *DoD Plane Wave: A General Scalable Density Functional Code*. 2002.
[16] Freeman, A.J., *Materials by design and the exciting role of quantum computation/simulation.* Journal of Computational and Applied Mathematics, 2002. **149**(1): p. 27-56.
[17] Rice, J. R. and Johnson, R, Inelastic Material Behavior, 1970
[18] Argon, A.S., J. Im, and A. Needleman, *Distribution of Plastic Strain and Negative-Pressure in Necked Steel and Copper Bars.* Metallurgical Transactions, 1975. **A 6**(4): p. 815-824.
[19] Hao, S. and Blocks, W., "The Gurson-Tvergaard-Needleman-Model for Rate and Temperature-Dependent Materials with Isotropic and Kinematic Hardening", Computational Mechanics, 20, 34-40.
[20]Rose, J.H., Smith, J.R., and Ferrante, J., *Universal features of bonding in metals.* Physical Review B, 1983. **28**(4): p. 1835-1845.